ChemComm

Non-conventional hydrogen bonding and dispersion forces that support embedding mesitylgold into a tailored bis(amidine) framework

Journal:	*ChemComm*
Manuscript ID	CC-COM-10-2021-006065.R2
Article Type:	Communication

COMMUNICATION

Non-conventional hydrogen bonding and dispersion forces that support embedding mesitylgold into a tailored bis(amidine) framework

Received 00th January 20xx,
Accepted 00th January 20xx

DOI: 10.1039/x0xx00000x

Janet Arras,[a] Omar Ugarte Trejo,[a] Nattamai Bhuvanesh [b] and Michael Stollenz *[a]

A bis(amidine) ligand operates as a molecular lock for two AuMes fragments. The resulting complex retains a flexible double macrocycle with two non-conventional N–H···C$_{ipso}$ hydrogen bonds and distinct intramolecular dispersion forces. Instead of unfolding of the double-ring structure through bond rupture in solution, a conformational ring inversion is observed.

Hydrogen bonds play a pivotal role in essential biological systems and generally as a dominant secondary bonding interaction in condensed phases.[1] The main focus has initially been on „classical" hydrogen bonding based on constituting electronegative donor and acceptor atoms such as N, O, or halogenides. Examples of usually weaker *non-traditional* hydrogen bonds include combinations of weak donor/weak hydrogen acceptors (X–H···π, X = C, Si, P, S, As, Se), weak donor/strong acceptors (predominantly X–H···O, X–H···N) or strong donor/weak acceptor atoms (N–H···X/π, O–H···X/π).[1c,d] Their effect on both molecular dynamics and structure-property relationships is still not well understood. However, there is strong evidence that the combination of these relatively weak intermolecular forces have a fundamental influence on supramolecular assemblies such as crystal packing and even biological structures[1c] –similar to significantly weaker London dispersion forces that have been in the focus of the more recent literature[2].

Within the category involving strong donor and weak acceptor atoms, non-conventional N–H···C and O–H···C hydrogen bonds have surfaced in only a limited number of experimental reports that recognize them as distinct bonding interactions.[3–7] Nevertheless, they have attracted considerable interest in fundamental studies such as infrared laser/microwave spectroscopic investigations on the methane-water complex[3], the role of N–H···C bonds in organolithium chemistry,[4] related solution-state and gas phase studies on carbanion[5] as well as isonitrile[6] hydrogen bonding, and also, more recently, their role as modulators in luminescent *N*-heterocyclic carbene/fluorophore adducts[7].

Herein we report an unusual dimesityl-digold bis(amidine) complex featuring intramolecular N–H···C hydrogen bonds that are supported by an ensemble of additional cooperative weak intramolecular forces that include C–H···Au,[8] C–H···N, C–H···C, and C–H···H–C[9] dispersive interactions, which are altogether contributing to the stabilization of a flexible double-macrocyclic ring system. The N–H···C bonding interactions indicate an onset of an incipient proton transfer reaction. We also demonstrate that such weak non-conventional secondary bonding interactions are retained in a dynamic molecular system and therefore serve as molecular locks for delicate organometallic fragments.

We have recently reported on a series of new *N*,*N*'-disubstituted ethylene-bridged bis(amidines) with additional terminal *N*-donor sites that exhibit unprecedented networks of weak to moderately strong inter- and intramolecular hydrogen bonds.[10] Our ongoing exploration of the coordination chemistry of these extremely flexible ligands has drawn our attention to the hexadentate bis(amidine) **L**H$_2$ (Scheme 1).

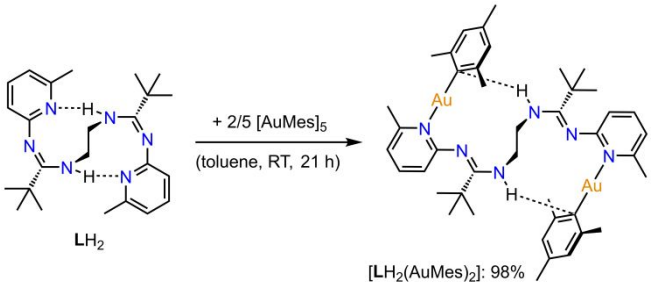

Scheme 1 Synthesis of complex [**L**H$_2$(AuMes)$_2$].

The C_2 symmetrical structure with two intramolecular N–H···N$_{Py}$ hydrogen bonds and two nine-membered rings in the bis(amidine) scaffold represents a tailored platform for structurally related dinuclear complexes. Our choice of mesitylgold[11] as synthon was inspired by its kinetic and thermodynamic stability, the absence of any co-ligand, its

[a] *Department of Chemistry and Biochemistry, Kennesaw State University 370 Paulding Avenue, MD 1203, Kennesaw, Georgia 30144, USA. E-mail: Michael.Stollenz@kennesaw.edu http://facultyweb.kennesaw.edu/mstollen/*
[b] *Department of Chemistry, Texas A&M University 580 Ross Street, P.O. Box 30012, College Station, Texas 77842-3012, USA.*
† Electronic Supplementary Information (ESI) available: Experimental procedures, computational details, crystallographic data and NMR spectra. CCDC 2105507 ([**L**H$_2$(AuMes)$_2$]). See DOI: 10.1039/x0xx00000x

excellent solubility in less polar organic solvents, the easy identification through only three diagnostic ^{1}H NMR signals, and ultimately the fact that stable related mixed coinage metal clusters exist for which mesitylgold serves as a convenient precursor.[12] Moreover, only a few mononuclear mesitylgold(I) complexes with additional stabilizing co-ligands are known.[12a,13]

The pentameric cluster $[AuMes]_5$ separates into distinct AuMes units upon coordination of **L**H_2, accompanied by a formal insertion into the hydrogen bonds of the bis(amidine) ligand. [**L**H_2(AuMes)$_2$] is formed in nearly quantitative yield (98%, Scheme 1). This dinuclear bis(amidine) complex possesses two non-conventional N–H···C_{ipso} hydrogen bonds completing two interconnected 11-membered rings. Variable-temperature (VT) ^{1}H NMR spectroscopy, accompanied by a comprehensive computational study, reveals a concerted double-ring inversion of [**L**H_2(AuMes)$_2$] that retains N–H···C_{ipso} hydrogen bonding in solution.

Single crystals of [**L**H_2(AuMes)$_2$] suitable for an XRD analysis were grown as colorless blocks from a slowly concentrating diethyl ether solution at room temperature and were found to crystallize in the triclinic spacegroup P$\bar{1}$. The unit cell shows one pair of C_2-symmetrical mirror-image conformations (Scheme 2, Electronic Supplementary Information, ESI, Fig. S3). One representative conformation is shown in Scheme 1.

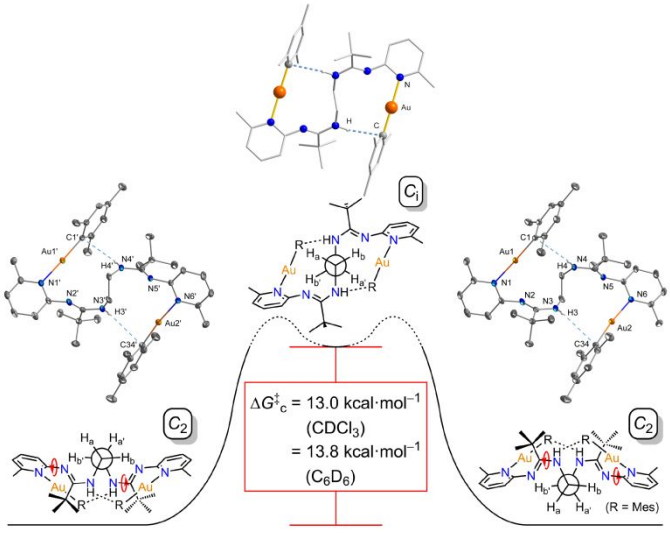

Scheme 2. Conformational inversion[14] of [**L**H_2(AuMes)$_2$] in solution with representations of the XRD-molecular structures of the two enantiomers of [**L**H_2(AuMes)$_2$] with C_2 symmetry (left and right) and the computational structure of the C_i-symmetrical intermediate (top)[15].

The two Au(I) centers exhibit linear coordination geometries, although with a larger deviation from linearity at Au2 (N6–Au2–C34 angle: 173.35(10)°) than at Au1 (N1–Au1–C1 angle: 177.4(1)°), presumably due to packing effects. The Au–N bonding distances of [**L**H_2(AuMes)$_2$] (2.102(2) Å and 2.111(2) Å) are significantly longer (by about 0.05–0.07 Å) than in related pyridine-type Au(I) complexes such as (2-MePy)AuCl (2.044(4) Å)[16a] and [(2-(NH_2)Py)AuCl] in [(2-(NH_2)Py)$_2$Au][(2-(NH_2)Py)AuCl][($AuCl_2$] (2.053(5) Å),[16b] which is attributed to the stronger trans influence of the mesityl ligands. Conversely, the Au–C bonds of [**L**H_2(AuMes)$_2$] (2.010(3) Å and 2.014(3) Å) are shorter in comparison to linear gold(I)mesityl complexes with stronger trans-stabilizing co-ligands than pyridyl in **L**H_2 such as phosphines in [MesAuP(Ph_2)(CH_2)$_2$(Ph_2)PAuMes] (2.067(6) Å),[11b] [MesAuP((3-Py)$_2$)(CH_2)$_2$((3-Py)$_2$)PAuMes] (2.067(4) Å),[12g] or [Ph_3PAuMes] (2.061(5) Å)[13a].

A remarkable feature of complex [**L**H_2(AuMes)$_2$] is the orientation of the mesityl ligands to the central –NH(CH_2)$_2$NH– diamine bridge. This orientation initially raised the question of whether there is hydrogen bonding between the NH donors and the π-system of the mesityl ligand. However, a closer inspection of the structure reveals significantly shorter N···C_{ipso} distances (3.525(4) Å and 3.647(4) Å) than to the next neighbored *ortho*-carbon atoms (by 0.25/0.41 Å and 0.09/0.80 Å, respectively), thus indicating two *discrete* N–H···C_{ipso} hydrogen bonds.[17,18] The donor-acceptor distances in [**L**H_2(AuMes)$_2$] are within the range of the weakest N–H···C contacts of a comparable example (3.594(9) Å).[4b] As expected for weak hydrogen bonds, these distances are also longer (by 0.58–0.72 Å) than in **L**H_2 that exhibits stronger N–H···N hydrogen bonding. However, the corresponding N–H···acceptor angles in [**L**H_2(AuMes)$_2$] (151(4)–153(4)°) are enlarged by 9–15° in comparison to the free bis(amidine) (see Table S4). These parameters agree with a classification of N–H···C_{ipso} weak hydrogen bonds,[17] which is supported by a slight red shift of the IR N–H stretching frequency of [**L**H_2(AuMes)$_2$] by 33 cm^{-1}, if compared to the bulky bis(amidine) {CH_2NH(^{t}Bu)C=N–Mes}$_2$[18] which does not show any hydrogen bonding (Fig. 1, Table S5).

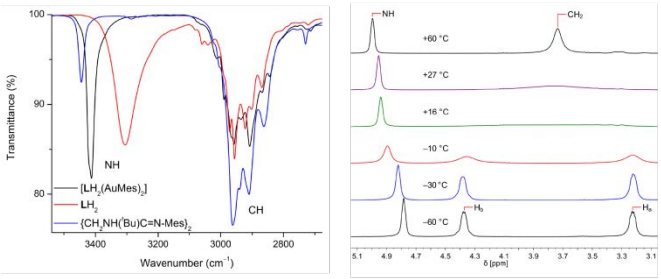

Fig. 1. Left: Region of NH and aliphatic CH stretching frequencies of the IR spectra of [**L**H_2(AuMes)$_2$], **L**H_2, and {CH_2NH(^{t}Bu)C=N–Mes}$_2$. Right: NH and CH_2 region of variable-temperature ^{1}H NMR spectra of [**L**H_2(AuMes)$_2$] in $CDCl_3$ (400 MHz).

This observation is consistent with the red-shifted calculated N–H bands of the computational geometry-optimized structure **I** in comparison to the computationally determined isomers **III** and **IV** that lack hydrogen bonding (*vide infra*, Scheme 3, and Table S7). The experimental N–H band at 3413 cm^{-1} reveals a shoulder which is in agreement with the slightly different N–H···C_{ipso} hydrogen bond lengths found in the crystalline state. Due to the anionic nature of the C_{ipso} donor atoms, the two N–H···C_{ipso} hydrogen bonds can be considered as *incipient proton transfer reactions* that would ultimately result in the formation of a bis(amidinate) and mesitylene. This controlled deprotonation represents an established and clean method for incorporating Cu^{I} ions by using more reactive mesitylcopper into homoleptic as well as heteroleptic alkoxide, amide, phosphide, and amidinate ligand scaffolds.[19–21]

A quantum theory of atoms in molecules (QTAIM) analysis[22] for [**L**H_2(AuMes)$_2$] shows bond critical points (BCPs) of the N–H···C_{ipso} bonds ($\rho(r_{BCP})$ = 0.0081/0.0070 eÅ^{-3}) and

small positive values for the Laplacian, $\nabla^2\rho(r_{BCP})$ = 0.0234/0.0203 eÅ^{-5}, that are indicative for interactions of dispersive character and comparable to C≡C–H···C(π) hydrogen bond electron densities.[23] The Bader charges at N (–1.1392/–1.1416) and C_{ipso} (–0.1632/–0.1618) suggest a weak, but significant polarization of the N–H···C_{ipso} bonds. In addition, there were overall 22 BCPs found for distinct supporting C–H···Au, C–H···N, C–H···C, and C–H···H–C dispersive interactions (Figs. S12–S14 and Tables S11–S12).

Next, we employed variable-temperature (VT) ^{1}H NMR spectroscopy to reveal the extraordinary stability of the double-macrocyclic ring system and the concerted molecular dynamics of [**L**H$_2$(AuMes)$_2$] (Fig. 1 and S23–S24). While almost all of the entire proton signals of [**L**H$_2$(AuMes)$_2$] remain unchanged across a wide temperature range and regardless of the solvent polarity ($CDCl_3$ or C_6D_6), there is a remarkable change in the CH_2 region. Decreasing temperature results in increasing line broadening, followed by decoalescence, and then separation into two singlets ($CDCl_3$: T_c = 16.5 °C; C_6D_6: T_c = 36.0 °C). The decoalescence in $CDCl_3$ is initially accompanied by increased line broadening of the downfield-shifted CH_2 signal relative to the upfield-shifted signal, which is indicative for the H_b protons that are in closer proximity to the bis(amidine) binding pockets (visible below about –10 °C, Fig. 1, right, and Fig. S23). A low-temperature NOESY experiment (–60 °C) confirmed the assignment to two proton signals H_a and H_b through the different intensity of the H_a/NH and H_b/NH crosspeaks (Fig. S25). In addition, splitting into apparent doublets indicate geminal coupling between the H_a and H_b nuclei at –60 °C ($|^2J_{HH}|$ = 4.3 Hz).

There is *no* significant shift of the N–H resonance associated with this dynamic process,[24] which is consistent with a concerted conformational inversion of the double 11-membered ring system that *retains* the two N–H···C_{ipso} hydrogen bonds (Scheme 2). An alternative disruption of hydrogen bonding would be expected to result in an upfield-shifted N–H resonance signal.[25] This inversion leads to a reversible interconversion from one C_2-symmetrical enantiomer into the other through the formation of an intermediate possessing C_i symmetry and is associated with free energies of activation for [**L**H$_2$(AuMes)$_2$] of $\Delta G_c^{\ddagger}$ = 13.0 kcal mol^{-1} in $CDCl_3$ and 13.8 kcal mol^{-1} in C_6D_6. DFT gas phase calculations confirm that the proposed C_i-symmetric intermediate (**II**) is higher in free energy by ΔG = +11.2 kcal mol^{-1} than the computationally-optimized molecular structure of [**L**H$_2$(AuMes)$_2$] (**I**, see ESI for details, Scheme 3, and Fig. S4). Both the experimental and calculated results are in agreement with this dynamic behavior rather than a mechanism involving disruption of hydrogen bonding. Such alternative isomers are shown in Scheme 3. The two proposed isomers of [**L**H$_2$(AuMes)$_2$], **III** and **IV** that lack hydrogen bonding correspond to the C_2-groundstate symmetry **I** (**III**) and to the C_i-symmetrical intermediate **II** (**IV**). This finding not only rule out an interconversion mechanism that involves separation of hydrogen bonds, but also confirms their extraordinary stability in conjunction with the insulating scaffold of [**L**H$_2$(AuMes)$_2$] at elevated temperatures, as substantiated by the essentially unchanged N–H ^{1}H NMR shifts at +60 °C in $CDCl_3$ (Fig. 1, Fig. S23) and at +75 °C in C_6D_6 (Fig. S24).[24]

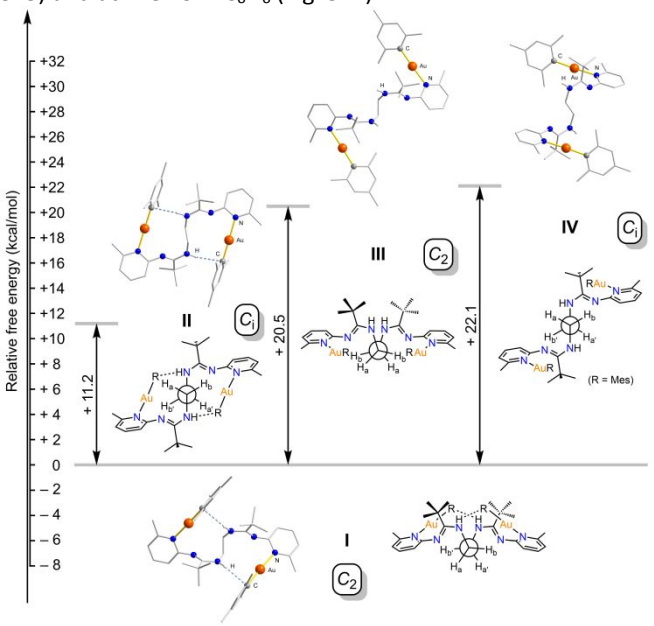

Scheme 3. Computationally determined isomers of [**L**H$_2$(AuMes)$_2$]: Geometry-optimized ground state (**I**), intermediate of the conformational ring inversion (**II**), and alternative isomers without hydrogen bonds (**III** and **IV**).[15] See ESI for details.

In conclusion, we have demonstrated that the *N*,*N*'-disubstituted ethylene-bridged bis(amidine) **L**H$_2$ with additional terminal *N*-donor sites is capable of incorporating distinct mesitylgold fragments of the [AuMes]$_5$ cluster into its pyridyl/amidine binding pockets. This results in the formation of the unique dinuclear complex [**L**H$_2$(AuMes)$_2$] which features a network of two non-conventional N–H···C_{ipso} hydrogen bonds and supporting London dispersion interactions that is retained in solution and constitutes a flexible double macrocycle. The two hydrogen bonds represent rarely observed primal onsets of proton transfers in an organometallic complex. VT-temperature studies in conjunction with DFT- gas phase calculations strongly support a dynamic conformational interconversion between two C_2-symmetrical ground states rather than a mechanism that unfolds the compact complex ensemble through bond rupture. These fundamental insights in the nature of weak non-conventional hydrogen bonds and London dispersion forces have implications on revisiting sole steric effects in supramolecular structures and reaction mechanisms, in particular those involving organometallic species in catalytic transformations.

Current studies focus on embedding other coinage metal fragments into bis(amidines) such as **L**H$_2$ to expand the scope to a systematic study of conventional and non-conventional hydrogen bonding interactions in these dynamic moieties.

We thank Allan Nguyen for experimental assistance, Dr. Andreas Ehnbom, Texas A&M University, for helpful discussions on computational work, and Prof. John Haseltine, Kennesaw State University, for reviewing an early version of this manuscript. The authors gratefully acknowledge support for providing computing resources by the Advanced Computer Services at Kennesaw State University and by the State of

Baden-Württemberg (Germany) through bwHPC, as well as financial support by the US National Science Foundation (CHE-1800332), Kennesaw State University, and Aditya Birla Carbon (Birla Carbon Scholarship for O.U.T.). There are no conflicts to declare.

Notes and references

1 (a) G. A. Jeffrey and W. Saenger, *Hydrogen Bonding in Biological Structures*, Springer, Berlin, 1991. (b) G. A. Jeffrey, *An Introduction to Hydrogen Bonding*, Oxford University Press, New York, 1997; (c) G. R. Desiraju and T. Steiner, *The Weak Hydrogen Bond in Structural Chemistry and Biology*, Oxford University Press, New York, 1999; (d) I. Alkorta, I. Rozas and J. Elguero, *Chem. Soc. Rev.*, 1998, **27**, 163–170; (e) T. Steiner, *Angew. Chem. Int. Ed.*, 2002, **41**, 48–76; (f) S. J. Grabowski, *Hydrogen Bonding - New Insights*, Springer, New York, 2006; (g) G. Gilli and P. Gilli, *The Nature of the Hydrogen Bond*, Oxford University Press, Oxford, U.K., 2009.

2 (a) J. P. Wagner and P. R. Schreiner, *Angew. Chem. Int. Ed.,* 2015, **54**, 12274–12296; (b) D.J. Liptrot and P. P. Power, *Nat. Rev. Chem.,* 2017, **1,** 0004, 1–12;(c) T. Schnitzer, T.; E. Paenurk, N. Trapp, R. Gershoni-Poranne and H. Wennemers, *J. Am. Chem. Soc.*, **2021**, **143**, 644−648.

3 (a) L. Dore, R. C. Cohen, C. A. Schmuttenmaer, K. L. Busarow, M. J. Elrod, J. G. Loeser and R. J., Saykally, *J. Chem. Phys.*, 1994, **100**, 863–876; (b) R. D. Suenram, G. T. Fraser, F. J. Lovas and Y. Kawashima, *J. Chem. Phys.*, 1994, **101**, 7230–7240.

4 (a) T. Laube, J. D. Dunitz and D. Seebach, *Helv. Chim. Acta*, 1985, **68**, 1373–1393; (b) S. Buchholz; K. Harms, M. Marsch, W. Massa and G. Boche, *Angew. Chem., Int. Ed. Engl.*, 1989, **28**, 72–73; (c) S. Buchholz, K. Harms, W. Massa and G. Boche, *Angew. Chem., Int. Ed. Engl.* 1989, **28**, 73–74.

5 (a) P. Ahlberg, B. Johnsson, I. McEwen and M. Rönnqvist, *J. Chem. Soc., Chem. Commun.*, **1986**, 1500–1501; (b) I. McEwen and P. Ahlberg, *J. Chem. Soc., Chem. Commun.*, **1989**, 1198–1199.

6 (a) P. v. R. Schleyer and A. Allerhand, A. *J. Am. Chem. Soc.*, 1962, **84**, 1322–1323; (b) L. L. Ferstandig, *J. Am. Chem. Soc.*, 1962, **84**, 3553–3557.

7 (a) J. A. Cowan, J. A. C. Clyburne, M. G. Davidson, R. L. W. Harris, J. A. K. Howard, P. Küpper, P., M. A. Leech and S. P. Richards, *Angew. Chem., Int. Ed.* 2002, **41**, 1432–1434; (b) J. M. Kieser, Z. J. Kinney, J. R. Gaffen, S. Evariste, A. M. Harrison, A. L. Rheingold and J. D. Protasiewicz, *J. Am. Chem. Soc.*, 2019, **141**, 12055–12063; (c) Z. J. Kinney, A. L. Rheingold and J. D. Protasiewicz, *RSC Adv.* 2020, **10**, 42164–42171.

8 C–H···Au bonds have been substantiated only recently: (a) Md. A. Bakar, M. Sugiuchi, M. Iwasaki,; Y. Shichibu, K. Konishi, *Nat. Commun.*, 2017, **8**, 576. (b) M. Rigoulet, S. Massou, E. D. Sosa Carrizo, S. Mallet-Ladeira, A. Amgoune, K. Miqueu and D. Bourissou, *Proc. Natl. Acad. Sci. USA*, 2019, **116**, 46–51. (c) M. Straka, E. Andris, J. Vícha, A. Růžička, J. Roithová, L. Rulíšek, *Angew. Chem. Int. Ed.* 2019, **58**, 2011–2016. (d) L. Estévez, L. *Dalton Trans.* 2020, **49**, 4797–4804.

9 H···H bonds have been verified by QTAIM bond paths: C. F. Matta, J. Hernández-Trujillo, T.-H. Tang, R. F. W. Bader, *Chem. Eur. J.*, 2003, **9**, 1940–1951.

10 C. O'Dea, O. Ugarte Trejo, J. Arras, A. Ehnbom, N. Bhuvanesh and M. Stollenz, *J. Org. Chem.*, 2019, **84**, 14217−14226.

11 (a) S. Gambarotta, C. Floriani, A. Chiesi-Villa and C. A. Guastini, *J. Chem. Soc., Chem. Commun.*, **1983**, 1304−1305; (b) E. M. Meyer, S. Gambarotta, C. Floriani, A. Chiesi-Villa and C. A. Guastini, *Organometallics*, 1989, **8**, 1067−1079; (c) R. Usón, A. Laguna, E. J. Fernández, M. E. Ruiz-Romero, P. G. Jones and J. Lautner, *J. Chem. Soc., Dalton Trans.*, **1989**, 2127−2131.

12 (a) M. Contel, J. Jiménez, P. G. Jones, A. Laguna and M. Laguna, *J. Chem. Soc., Dalton Trans.*, **1994**, 2515−2518; (b) M. Contel, J. Garrido, M. C. Gimeno, P. G. Jones, A. Laguna and M. Laguna, *Organometallics*, 1996, **15**, 4939−4943; (c) M. Contel, J. Garrido, M. C. Gimeno, J. Jiménez, P. G. Jones, A. Laguna and M. Laguna, *Inorg. Chim. Acta*, 1997, **254**, 157−161; (d) E. Cerrada, M. Contel, A. D. Valencia, M. Laguna, T. Gelbrich and M. B. Hursthouse, *Angew. Chem., Int. Ed.*, 2000, **39**, 2353–2356; (e) M. Laguna, J. Garrido and M. Contel, *Inorg. Synth.*, 2002, **33**, 181–184; (f) E. J. Fernández, A. Laguna, J. M. López-de-Luzuriaga,; M. Montiel, M. E. Olmos, J. Pérez and R. C. Puelles, *Organometallics*, 2006, **25**, 4307–4315; (g) M. Frik, J. Jiménez, I. Gracia, L. R. Falvello, S. Abi-Habib, K. Suriel, T. R. Muth and M. Contel, *Chem. Eur. J.*, 2012, **18**, 3659–3674; (h) P. Ai, C. Gourlaouen, A. A. Danopoulos and P. Braunstein, *Inorg. Chem.*, 2016, **55**, 1219–1229.

13 (a) C. Croix, A. Balland-Longeau, H. Allouchi, M. Giorgi, A. Duchêne and J. Thibonnet, *J. Organomet. Chem.*, 2005, **690**, 4835–4843; (b) D. V. Partyka, J. B. Updegraff, M. Zeller, A. D. Hunter and T. G. Gray, *Organometallics*, 2009, **28**, 1666–1674; (c) D. V. Partyka, M. Zeller, A. D. Hunter and T. G. Gray, *Inorg. Chem.* 2012, **51**, 8394−8401; (d) S. Dupuy, L. Crawford, M. Bühl, A. M. Z. Slawin and S. P. Nolan, *Adv. Synth. Catal.*, 2012, **354**, 2380–2386.

14 Note that the transformation of C_2 to C_i results in an inversion of $H_{a'}$ to $H_{b'}$ and $H_{b'}$ to $H_{a'}$, (left entiomer to intermediate) as well as H_a to H_b and H_b to H_a, (right entiomer to intermediate), and vice versa.

15 Geometry optimizations were performed with TURBOMOLE at the level of theory of RIDFT-D3/B3LYP/def2-TZVP. Thermochemical corrections were calculated using Gaussian at the DFT-D3/BP-86/def2-SVP level of theory.

16 (a) P. G. Jones and B. Ahrens, *Z. Naturforsch. B*, 1998, **53**, 653−662; (b) J. H. K. Yip, R. Feng and J. J. Vittal, *Inorg. Chem.*, 1999, **38**, 3586−3589.

17 For criteria to categorize strong, moderately strong, and weak hydrogen bonds see Ref. 1b.

18 A. Calderón-Díaz, J. Arras, E. T. Miller, N. Bhuvanesh, C. D. McMillen and M. Stollenz, *Eur. J. Org. Chem.*, 2020, **22**, 3243–3250.

19 M. Stollenz, F. Meyer, *Organometallics*, 2012, **31**, 7708–7727.

20 M. Stollenz, J. E. Raymond, L. M. Pérez, J. Wiederkehr and N. Bhuvanesh, *Chem. Eur. J.*, 2016, **22**, 2396–2405.

21 M. Stollenz, *Chem. Eur. J.*, 2019, **25**, 4274–4298.

22 R. F. W. Bader, *Chem. Rev.*, 1991, **91**, 893–928.

23 S. J. Grabowski, J. M. Ugalde, *J. Phys. Chem. A*, 2010, **114**,7223–7229.

24 The NH proton signal shifts by $\Delta\delta$ = +0.22 ppm in $CDCl_3$ (–60 °C...+60 °C) and $\Delta\delta$ = –0.04 ppm in C_6D_6 (+60 °C...+75 °C). All other proton signals are shifted between $\Delta\delta$ = –0.10 ppm and +0.17 ppm ($CDCl_3$) as well as $\Delta\delta$ = –0.08 ppm and +0.13 ppm (C_6D_6) in the corresponding temperature ranges. See also Figs. S23 and S24, ESI.

25 For correlations between ^{1}H NMR chemical shifts and crystallographic data of hydrogen bonds see: (a) V. Bertolasi, P. Gilli, V. Ferretti and G. Gilli, *J. Chem. Soc., Perkin Trans. 2*, **1997**, 945–952; (b) T. K. Harris, Q. Zhao and A. S. Mildvan, *J. Mol. Struct.*, 2000, **552**, 97–109.